Journal of the Mechanical Behavior of Biomedical Materials 173 (2026) 107234

Contents lists available at ScienceDirect

Journal of the Mechanical Behavior of Biomedical Materials

journal homepage: www.elsevier.com/locate/jmbbm

Research paper

Comparative evaluation of the mechanical properties of amniotic membranes for corneal grafting: Effects of cryopreservation, lyophilization, and dehydration

B. Fantaci [a,*], B. Calvo [a,b], A.M. Mesa [c], A. Ortillés [c]

[a] Aragón Institute of Engineering Research (I3A), Universidad de Zaragoza. Zaragoza, Spain
[b] Centro de Investigación Biomédica en Red en Bioingeniería, Biomateriales y Nanomedicina (CIBER-BBN), Spain
[c] AniCura Valencia Sur Hospital Veterinario. Silla (Valencia)., Spain

ARTICLE INFO

Keywords:
Amniotic membranes
Mechanical behavior
Experimental test

ABSTRACT

In both human and veterinary ophthalmology, stromal to full-thickness corneal defects can be treated using several techniques that involve various biomaterials, which support healing while preserving vision. Among these, the amniotic membrane stands out due to its multifaceted biological properties, including anti-inflammatory, antimicrobial, and regenerative capabilities. Three main preservation methods (cryopreservation, dehydration, and lyophilization) have been developed to facilitate amniotic membrane clinical use. However, these methods may significantly alter its mechanical and structural integrity, which are critical for graft success. This study investigates the mechanical performance of bovine amniotic membranes for veterinary use, preserved using the above-mentioned techniques, by means of uniaxial tensile and inflation tests in a non-biological in vitro setting. Structural and chemical differences are also analyzed using scanning electron microscopy and energy-dispersive X-ray spectroscopy. Despite structural differences arose among the samples, these differences did not alter or worsen the structural resistance of the membranes. All samples withstood 5 inflation cycles of 200 mmHg without leaking.

1. Introduction

Each year, corneal ulcers affect millions of individuals (both humans and animals) globally, often leading to severe complications such as visual impairment or permanent blindness if left untreated (Byrd et al., 2024). It is estimated that 1.5 to 2 million new cases of corneal infections occur annually worldwide, predominantly in low- and middle-income countries where access to timely health care may be limited (Stapleton, 2023). The difficulty in managing this condition stems from the alarming increase in antibiotic resistance, the growing demand for corneal donors, and escalating costs associated with medical and surgical therapies (Stapleton, 2023).

Corneal ulceration is most likely caused by several etiologies including infectious, immune mediated and trauma (Stapleton, 2023; Maini et al., 2020; Hoerdemann and Yarbrough, 2023; Sanchez et al., 2024; Hassanpour et al., 2022; Ruiz-Lozano et al., 2023; Andrew, 2008; Braus et al., 2017). Consequently, significant efforts in clinical research are directed towards developing reliable and cost-effective solutions for repairing corneal defects, rather than resorting to keratoplasty, given the difficulty in recruiting donor corneas and the related cost.

In both human and veterinary ophthalmology, several techniques for corneal reconstruction have been described (Sanchez et al., 2024; Ledbetter et al., 2025). These techniques support healing while preserving vision and can be classified based on the material used: autologous ocular tissues (i.e., corneal or conjunctival grafts, and corneo-conjunctival transposition) and homologous and heterologous donor tissues (e.g., fresh or preserved corneal grafts) (Sanchez et al., 2024; Ledbetter et al., 2025); additionally, a less well-known category includes keratoprosthetics (Allgoewer et al., 2010). Biomaterials most commonly used for repairing stromal to full-thickness corneal defects in dogs, cats and horses are acellular cornea (Santillo et al., 2021), amniotic membrane (Costa et al., 2019), small intestinal submucosa (Goulle, 2012), and urinary bladder acellular matrix (Chow and Westermeyer, 2016). However, surgical success with others such as nictitating membrane and pinnal cartilage (Kanai et al., 2006; Mathes et al., 2015), tunica vaginalis (Vicenti et al., 2003), renal capsule (Andrade et al., 1999), buccal mucosa (Mezzadri et al., 2021), fascia lata (Hoerdemann and Yarbrough, 2023), omentum (Thajunnisa et al., 2020), pericardium (Dulaurent et al., 2014), peritoneum (Barros and

* Corresponding author.
E-mail address: bfantaci@unizar.es (B. Fantaci).

https://doi.org/10.1016/j.jmbbm.2025.107234
Received 1 September 2025; Received in revised form 6 October 2025; Accepted 16 October 2025
Available online 21 October 2025

Safatle, 2000), or platelet-rich fibrin membranes (Baadsgaard Bruun et al., 2025) has also been reported.

Among the various materials employed, the amniotic membrane (AM) stands out due to its multifunctional properties. Amnion is the innermost fetal layer of the placenta, composed by three different layers: monolayer columnar epithelium, basement membrane and avascular stroma (Jirsova and Jones, 2017). In addition to providing tectonic support, it has anti-inflammatory, anti-fibroblastic, anti-angiogenic, anti-protease and anti-microbial properties, promotes epithelization and exhibits immune-privilege (Jafari et al., 2024). Based on these properties, AM is currently used for a wide spectrum of ocular surface indications in humans, such as persistent corneal or conjunctival epithelial defects, chemical or thermal burns, limbal stem cell deficiency, cicatrizing conjunctivitis, ocular graft versus host disease, microbial keratitis, corneal perforation, bullous keratopathy, dry eye disease, corneal haze following refractive surgery and cross-linking, band keratopathy, ocular suIn veterinary ophthalmology, anatomic and visual success rates following AM grafting are high regardless of the preservation method used, with 93%–100% anatomic success and 85%–93% vision maintenance or restoration (Costa et al., 2019; Maini et al., 2020; Ledbetter et al., 2025). These studies have demonstrated that AM transplantation is a valuable tool in different ocular surface diseases such as non-healing corneal erosion, ulcers associated with tear deficiency or partial burn, and indolent ulcers (Arcelli et al., 2009), and for corneal surface reconstruction in keratomalacia (Costa et al., 2019; Maini et al., 2020), mid stromal to full-thickness defects (Costa et al., 2019; Maini et al., 2020; Dower et al., 2022), dystrophy (Lassaline-Utter et al., 2014), after excision of sequestrum (Barachetti et al., 2010; Gómez et al., 2023; Maini et al., 2020), dermoids (Kalpravidh et al., 2009), epithelial inclusion cysts (Cassagnes et al., 2020), fibrous histiocytoma (Barros et al., 2005) or corneolimbal squamous cell carcinomas (Ollivier et al., 2006).

Amnion can be applied either epithelial side up (i.e., inlay technique) as a scaffold for migrating epithelial cells over the membrane and to facilitate graft integration, or stromal side up (i.e., overlay technique) as a patch to cover lesions without graft integration and for protecting the corneal surface (Malhotra and Jain, 2014). Depending on the depth, the former technique may be used as a single layer graft inlay or a multilayer graft inlay where these layers are placed into the ulcer ground without sutures before a outermost graft is sutured to its periphery (i.e., layered or fill in technique). This may be done either by cutting the amnion into multiple pieces and placing them one on top of one another or by repeatedly folding upon itself a larger piece (blanket fold). Both inlay and overlay techniques can also be combined using two or more layers with the inner smaller layer acting as a graft and the outer larger layer as a patch (i.e., sandwich technique) (Malhotra and Jain, 2014).

Three main preservation methods are currently used to store AMs (Jirsova and Jones, 2017): cryopreservation, dehydration (air, heat or low-temperature vacuum-drying) and lyophilization (freeze-drying). However, since preservation and storage methods can change AM biological features, and also its structural and mechanical properties (Jafari et al., 2024), significant efforts in clinical research are directed towards developing reliable and cost-effective solutions for achieving optimal biomaterial storage and shipping without substantial alteration of their whole properties. These variations are critical to understanding how AM behaves when transplanted for corneal defect repair, and how they influence the grafts success.

The aim of the study was to investigate the mechanical behavior of bovine amniotic membranes preserved through different methods in a non-biological in vitro model through uniaxial and inflation tests and to assess the ultrastructural changes among the methods using scanning electron microscopy (SEM). Moreover, energy dispersive X-ray spectroscopy (EDX) was used to check the chemical composition of the AMs. By comparing cryopreserved (CAM), lyophilized (LAM), and dehydrated (DAM) amniotic membranes, this study seeks to provide insights into the most suitable preservation technique for maximizing the structural integrity of AM in corneal grafting procedures.

Table 1
Average strip thickness, width and length values [mm ± std] of the samples, after hydration.

	Thickness	Width	Length
CAM	0.11 ± 0.00	3.10 ± 0.31	12.30 ± 2.37
LAM	0.03 ± 0.00	3.93 ± 0.22	10.99 ± 1.65
DAM	0.03 ± 0.00	3.28 ± 0.07	15.33 ± 1.03
LAM-2	0.02 ± 0.00	4.90 ± 0.00	10.99 ± 1.39
DAM-2	0.02 ± 0.00	1.50 ± 0.35	9.41 ± 2.76

2. Materials and methods

In this study, three amniotic membranes from the same lot (CAM, LAM and DAM; AMNIOVET^{TM}, VetBiologicals, Valencia, Spain) were tested through two mechanical experimental tests (uniaxial tension test and inflation test) and structurally analyzed by SEM and EDX.

2.1. Sample preparation

Before performing the mechanical tests, each membrane was prepared following manufacturer's recommendations. CAMs were stored at −20°, while DAMs and LAMs were kept at room temperature. Before testing, CAMs were thawed by warming the sealed package in lukewarm water for 10 min.

Two different protocols were tested to hydrate the LAMs and DAMs samples: first, the samples were submerged in 3 ml of a balanced salt solution (BSS) for 5 min (referred as LAM and DAM); then, the protocol was changed and the samples (referred as LAM-2 and DAM-2) were rehydrated by first submerging them in 3 ml BSS for 3 min and then in a specific restorative solvent provided by the manufacturer for 2 more minutes.

2.2. Uniaxial tension test

For each AM type, four dog-bone-shaped specimens were punched out to be tested. On a white protective plastic base, after removing the package, the membrane was flattened, and a central fragment was cut. The membrane strips were clamped vertically between the jaws and uniaxial tensile tests were performed under displacement control on an Instron 5548 Microtester (Illinois Tool Works Inc., Glenview, USA) with a 10 N full scale load cell (Fig. 1). To avoid specimen drying, an ultrasonic humidifier was used, which provided a subcooling steam and kept a constant temperature of 25 °C. A testing velocity estimated as 5 mm/min was maintained throughout the test and for all specimens. Load and displacement were recorded until complete sample rupture. Strip elongation was expressed by the stretch, calculated as $\lambda = (L_0 + \Delta L)/L_0$, where L_0 is the initial length between clamps and Δ L is the upper clamp displacement. The failure Cauchy stress was obtained as $\sigma = (N\lambda)/CSA$, where N is the applied load and CSA is the initial cross-sectional area of the specimen. All the curves were truncated before complete failure of the sample at a strain around 20%–30% and the mean curve was obtained afterwards.

The average strip thickness, width and length between the jaws values (± standard deviation (std)) of the three AMs, once hydrated, are shown in Table 1.

2.3. Inflation test

To perform the inflation test, square shaped samples of the AMs were cut and placed in a specifically designed 3D chamber (Fig. 2.a–b), closed with screws to avoid undesired pressure variations or liquid leakage. The chamber had an internal diameter of 15 mm.

The inflation test consisted of injecting 2 ml/min of water inside the camera and pressure sensor was placed to measure the pressure inside the camera. Two samples for each membrane type were tested

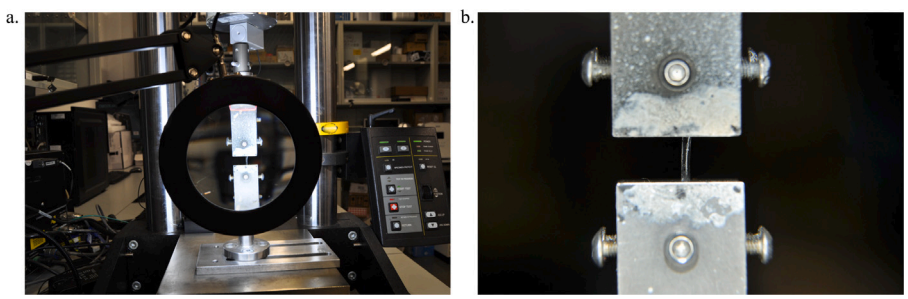

Fig. 1. Experimental set up for the uniaxial test. a. experimental set up; CAM sample undergoing uniaxial test.

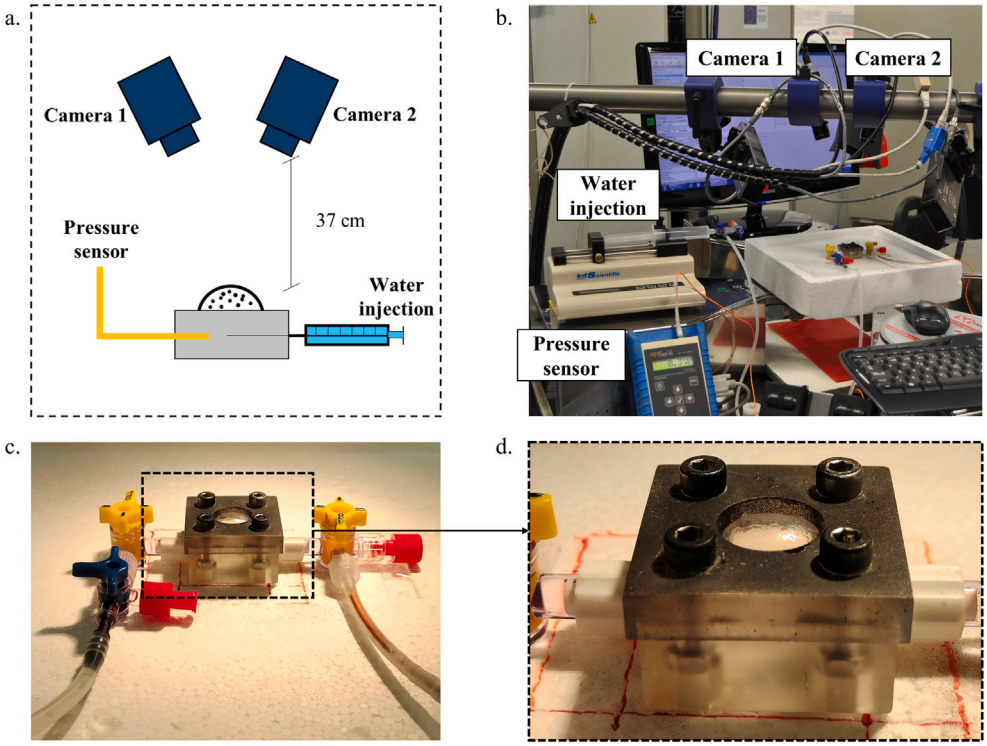

Fig. 2. Experimental set up for the inflation test. a. schematic of the experimental set up; b. experimental set up; c. chamber for the inflation test with two inlets (one for the pressure sensor and another for the water injection); d. zoomed view on the chamber during CAM's inflation test.

and five cycles from 0 to 200 mmHg were carried out for each sample. Therefore, 10 tests were performed for each membrane type. The entire procedure was recorded using a Digital Image Correlation (DIC) system (Fig. 2.a–b).

The DIC system consists of two cameras (Imager E Lite, LaVision, Germany) and a desktop computer with a Quad-core processor. The cameras had a spatial resolution of 1280 × 1024 pixels and a maximum frame rate of 500 fps. The cameras were placed at a distance of approximately 37 cm from the chamber and the mutual distance between cameras was approximately 13 cm. Both cameras were mounted with an identical 200 mm f/4 lens (Nikon, Tokyo, Japan) with an opening angle of approximately 30°. The two cameras were internally synchronized with LaVision software and high-power light-emitting diodes (LEDs) fed with distensibility coefficient (DC) to avoid flickering illuminated the sample. Automatic system calibration by LaVision software was performed with a grid pattern before conducting the inflation tests. DIC requires the presence of a random pattern on the specimen. This was achieved by applying black spray paint on top of the samples. LaVision software generated 4 images/s .vc7 files in each test. These files were processed with the PIVMat 4.20 Toolbox21 in MATLAB R2024a and contained both the reference coordinates and the 3D displacement (u_x, u_y and u_z) of the correlated speckle pattern; in this work, the central point of the membrane has been considered. For each curve, only the interval between 0 and 45 mmHg was considered and the mean curve for each AM type was calculated.

2.4. Ultrastructural analysis with SEM and EDX

AM samples were prepared for SEM analysis. Different preparation protocols were followed depending on the type of AM. Being already dehydrated, LAM and DAM samples did not need any fixation procedure and were directly coated with platinum (Pt) (Zhang et al., 2016) with 40 mA for 60 s. Finally, the samples were examined with a field emission scanning electron microscope (FE-SEM) (MERLIN^{TM}, Carl Zeiss, Oberkochen, Germany).

Given the water content, the CAM samples had to follow a different preparation prior to the observation with the SEM. Fixation of the sample was performed using a 4% paraformaldehyde and 2.5% glutaraldehyde solution in PBS. The samples were then washed with phosphate buffer (PBS 0.1 M) (five times for five minutes each). Post-fixation was carried out with 1% osmium tetroxide in PBS for 1 h. Following this, the samples were washed with milli-Q water (three times for five minutes each). Dehydration was achieved using ethanol

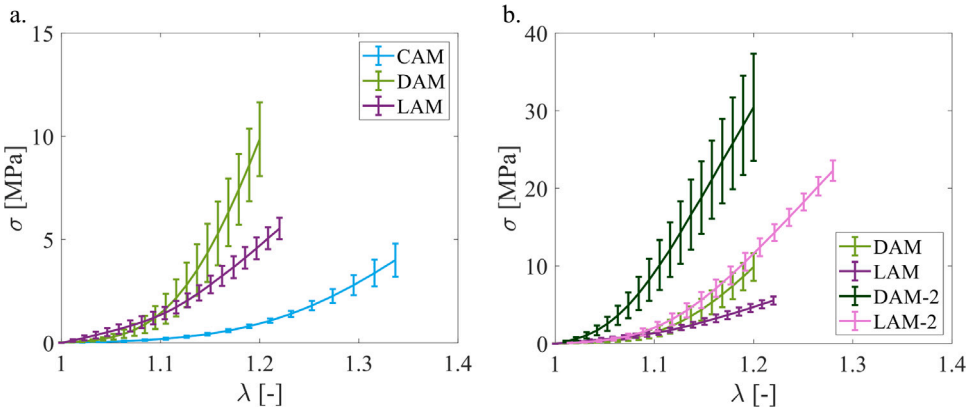

Fig. 3. Uniaxial tension test. a. Curves of the uniaxial tests of CAM, DAM and LAM sample; b. Comparison of the curves of uniaxial test of DAM and LAM samples, that followed two different preparation protocols.

Table 2
Average stress values (MPa ± std) for 5%, 10%, 15% and 20% strain.

Strain (Stretch)	CAM	LAM	DAM	LAM-2	DAM-2
5% (λ = 1.05)	0.06 ± 0.03	0.59 ± 0.23	0.23 ± 0.11	0.44 ± 0.15	1.45 ± 0.92
10% (λ = 1.10)	0.18 ± 0.05	1.38 ± 0.35	1.27 ± 0.61	2.06 ± 0.57	5.82 ± 2.89
15% (λ = 1.15)	0.44 ± 0.08	2.82 ± 0.49	4.24 ± 1.38	5.89 ± 1.04	13.66 ± 5.62
20% (λ = 1.2)	0.94 ± 0.11	4.68 ± 0.61	9.45 ± 1.74	11.65 ± 1.17	22.36 ± 7.89

at increasing concentrations: 30% (1 × 5 min), 50% (1 × 5 min), 70% (2 × 5 min), 96% (2 × 10 min), and 100% (3 × 10 min). Subsequently, a total water adsorption procedure was performed by submitting CAM samples to a critical point drying stage (Leica EM CPD300 Critical Point Dryer, Germany). The samples were then mounted on SEM (JEOL JSM 6360-LV) supports and coated with gold and palladium (Au/Pd) using a BALTEC SCD-005 coater to enhance the samples' conductivity and produce clearer images during the electron microscopy process.

To check the chemical composition of the AMs, EDX was used to examine the membranes.

2.5. Statistical analysis

A statistical analysis was performed to assess whether the observed behaviors were statistically significant. For the uniaxial tension tests, Cauchy stress values at stretches λ = 1.05, 1.10, 1.15, 1.20 (i.e., 5%, 10%, 15% and 20% strain, respectively; mean ± SD) were calculated for all samples. After acquiring the stress–stretch curves of individual samples, curves were averaged to obtain the mean response of each group. For the inflation tests, apical displacements at 2.5, 5, 10, 15, 20, 25, 30, 35, 40 and 45 mmHg were extracted to construct apical displacement–IOP curves. For each sample, one curve per cycle was acquired; the five cycles of the same sample were averaged, and then sample means were averaged within each membrane type to obtain the group mean response.

The statistical analysis was carried out in SPSS 19.0 (SPSS Inc., Chicago, USA). Data were reorganized in long format by Group (CAM, LAM, DAM, LAM-2, DAM-2), Specimen ID, Level (stretch for uniaxial; pressure for inflation) and Response. Normality of continuous variables within groups was evaluated using the Kolmogorov–Smirnov test with Lilliefors correction; homoscedasticity was assessed with Levene's test. Two-sided $p < 0.05$ was considered statistically significant. For each level of stretch (λ) or pressure (IOP), between-group differences were first assessed with an omnibus test: one-way ANOVA when distributional assumptions (normality and homoscedasticity) held and Kruskal–Wallis test otherwise. When the omnibus test was significant, post-hoc pairwise comparisons were conducted using Tukey's HSD (after ANOVA) or Dunn–Šidák (after Kruskal–Wallis) to compare Cauchy stress (σ) and apical displacement between groups.

In addition, to evaluate overall differences along the entire curves (accounting for repeated measures within specimens), linear mixed-effects models were fitted with fixed effects for group, level, and their interaction, and random effects for specimens nested within group.

3. Results

3.1. Uniaxial tension test

All the AM samples showed a non-linear behavior when subjected to uniaxial tests (Fig. 3). For each curve, three major regions can be distinguished: (1) the toe region represents "un-crimping" of the collagen fibrils, (2) the linear region, where the collagen fibrils become uncrimped and they begin to stretch making the tissue stiffer, and (3) the yield and failure region, where the accumulation of damage due to individual fibril failure causes loss of stiffness, and then the tissue begins to fail (this region is not displayed). First, a comparison of CAM, DAM, and LAM samples subjected to the first protocol was performed (Fig. 3.a). Then, the preparation protocol was changed for DAM and LAM only (namely DAM-2 and LAM-2), and the curves were compared with the curves from the previous protocol (Fig. 3.b). Table 2 shows the average stress values for 5%, 10%, 15% and 20% strain and Table 3 shows the p-values of the statistical analysis between the AM samples.

The softest behavior was shown by CAM samples, that had a failure stress of around 4 ± 0.8 MPa for a strain around 34%. DAM samples showed the stiffest behavior with a failure stress of 9.86 ± 1.79 MPa, while LAM samples had an intermediate behavior with a stress failure of 5.54 ± 0.52 MPa.

Following the statistical analysis, adjusted pairwise p-values (Tukey or Dunn–Šidák, as appropriate) are reported in Table 3. Significant differences were found between CAM and LAM, and between CAM and DAM at the highest stretch levels (λ = 1.15 – 1.20). LAM and DAM differed significantly only at λ = 1.20.

When the second protocol was applied to DAM and LAM samples, they both showed a stiffer behavior with respect to the samples that were subjected to the previous protocol (Fig. 3.b), reaching a failure stress three and four times higher, respectively ($\sigma_{DAM\text{-}2}$ = 30.45 ± 6.9 at a 20% strain, $\sigma_{LAM\text{-}2}$ = 22.28 ± 1.3 at a 30% strain). LAM-2 samples failed at a strain 10% higher than LAM, demonstrating greater resistance. Significant differences were detected between CAM and LAM-2

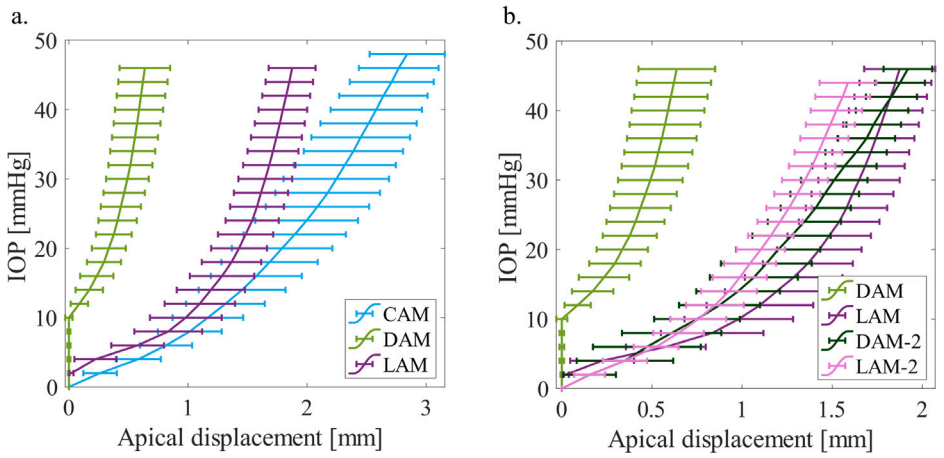

Fig. 4. Inflation test. a. Curves of the inflation tests of CAM, DAM and LAM samples; b. Comparison of the curves of inflation test of DAM and LAM samples, that followed two different preparation protocols.

Table 3
Statistical analysis of the AM samples that underwent uniaxial test at stretch $\lambda = 1.05, 1.10, 1.15, 1.20$. The table reports adjusted pairwise p-values (Tukey or Dunn–Šidák) at each stretch level.

	1.05	1.10	1.15	1.20
CAM - LAM	0.112	0.033*	0.010*	0.005*
CAM - DAM	0.190	0.124	0.046*	0.010*
LAM - DAM	0.190	0.750	0.132	0.024*
CAM - LAM-2	0.023*	0.011*	0.002*	0.0001*
CAM - DAM-2	0.157	0.065	0.029*	0.015*
LAM - LAM-2	0.255	0.128	0.006*	0.0001*
LAM - DAM-2	0.190	0.108	0.046*	0.024*
DAM - LAM-2	0.190	0.128	0.132	0.054
DAM - DAM-2	0.190	0.108	0.048*	0.040*
LAM-2 - DAM-2	0.190	0.124	0.074	0.053

* Statistically significant differences ($p < 0.05$).

at all stretches. Most other pairwise contrasts became significant only at higher stretches (λ = 1.15–1.20, Table 3). No significant differences were observed between DAM and LAM-2 or between LAM-2 and DAM-2. Overall, group differences increased with stretch, with DAM-2 consistently showing higher stress than CAM, LAM, and DAM.

Consistent with the curve trends, mixed-effects modeling of the stress–stretch data confirmed a significant effect of Level and of group-dependent evolution with loading (Group×Level, i.e., curve slopes differed between groups), indicating group-dependent changes in stiffness with increasing stretch. These global findings are consistent with the per-level contrasts reported in Table 3.

3.2. Inflation test

For each cycle, all the AM samples withstood a maximum pressure of 200 mmHg without rupture or leakage. For the inflation test as well, all the AM samples exhibited non-linear behavior, similarly to what was observed in the uniaxial tension tests. CAM had the highest apical displacement during the tests (2.74 ± 0.34 at 45 mmHg, Table 4), confirming to have the softest behavior, as observed in the uniaxial tests. On the other hand, DAM samples had the lowest apical displacement (0.63 ± 0.21 at 45 mmHg, Table 4), being the stiffest among the three AM types. Following the statistical analysis (Table 5), CAMs and LAMs were significantly more compliant than DAMs from 5 to 45 mmHg ($p < 0.05$), without statistically significant differences between CAM and LAM samples ($p < 0.05$).

Differently from the uniaxial test, where the stiffening effect of the second protocol on DAM and LAM samples was clear, for the inflation test mixed results were obtained. While LAM samples stiffened when they were subjected to the second protocol (LAM-2 in Fig. 4.b), DAM samples underwent a softening of the mechanical properties, after the second protocol was applied, when subjected to the inflation test. While DAM samples were considerably stiffer with respect to the other samples (apical displacement of 0.63 ± 0.21, Table 4), the behavior of DAM-2, LAM and LAM-2 was comparable in terms of apical displacement. Returning to the statistical analysis, DAM samples were found to be statistically different with respect to both LAM-2 and DAM-2 ($p < 0.05$). Significant differences were also found between CAM and LAM-2 only for pressure values of 35, 40 and 45 mmHg and between LAM-2 and DAM-2 at 40 and 45 mmHg. LAM and LAM-2 were found to be statistically different for pressure values from 10 to 30 mmHg and no differences were found between CAM and DAM-2 and between LAM and DAM-2 ($p > 0.05$, Table 5).

Mixed-effects modeling of the apical displacement–IOP data confirmed a strong effect of Level and evidence of group-dependent evolution with loading (Group×Level), i.e., pressure–displacement curve slopes differed between groups. These global findings are consistent with the per-level contrasts reported in Table 5.

3.3. Ultrastructural analysis with SEM

The AM samples were analyzed with the SEM to show detailed changes between CAM, LAM and DAM structure due to the preservation process. Since the AM samples were prepared using different protocols and examined with multiple instruments, the CAM samples were first analyzed individually, followed by a comparison of the DAM and LAM samples. Magnifications of 50×, 100×, 500×, 1000× and 5000× were considered for each sample; however, we report only 100×, 1000× and 5000× for the CAM sample and 100× and 1000× for the DAM and LAM samples to avoid redundancy.

The dried CAM samples appeared to be compact and homogeneous (Fig. 5). At 1000× magnification, wrinkles were noticeable, likely due to the fixation process, which also caused the removal of a thin film layer (probably the epithelium), as seen in the upper-left edge of the 100× magnification image and that could be visible in other areas of the sample, that are not here reported. At 5000× magnification, centered near the cut edge of the sample, a fibrous structure was observed, probably constituting the collagen fibers of the stroma of the AM.

Since the DAM and LAM samples were prepared using the same protocol and examined with the field emission scanning electron microscope (FE-SEM), they were directly compared. Unlike the CAM samples, where the reference to each side is lost during the preparation process due to the complete submersion of the sample, it was possible to keep track of each side of the DAM and LAM samples throughout preparation and examination (Fig. 6). DAM appeared to be the most homogeneous

Table 4
Average apical displacements values (mm ± std) for different IOP values.

IOP [mmHg]	CAM	LAM	DAM	LAM-2	DAM-2
5	0.69 ± 0.21	0.43 ± 0.20	0.01 ± 0.01	0.44 ± 0.11	0.42 ± 0.29
15	1.52 ± 0.37	1.24 ± 0.28	0.21 ± 0.14	0.96 ± 0.15	1.02 ± 0.24
25	2.04 ± 0.44	1.56 ± 0.22	0.42 ± 0.16	1.24 ± 0.12	1.38 ± 0.20
35	2.42 ± 0.42	1.73 ± 0.21	0.54 ± 0.19	1.44 ± 0.13	1.66 ± 0.16
45	2.74 ± 0.34	1.86 ± 0.20	0.63 ± 0.21	1.60 ± 0.16	1.90 ± 0.14

Table 5
Statistical analysis of the AM samples that underwent inflation test at pressure values from 5 to 45 mmHg. The table reports adjusted pairwise p-values (Tukey or Dunn–Šidák) at each IOP level.

	5	10	15	20	25	30	35	40	45
CAM - LAM	0.797	0.998	0.996	0.994	0.990	0.955	0.776	0.755	0.685
CAM - DAM	0.007*	0.007*	0.007*	0.003*	0.003*	0.002*	0.001*	0.001*	0.001*
LAM - DAM	0.141	0.013*	0.017*	0.007*	0.009*	0.017*	0.033*	0.036*	0.050*
CAM - LAM-2	0.724	0.508	0.423	0.142	0.099	0.077	0.031*	0.029*	0.026*
CAM - DAM-2	0.817	0.511	0.661	0.415	0.586	0.661	0.685	0.732	0.817
LAM - LAM-2	0.060	0.029*	0.013*	0.014*	0.028*	0.051	0.082	0.114	0.154
LAM - DAM-2	0.567	0.271	0.316	0.392	0.599	0.850	0.684	0.594	0.486
DAM - LAM-2	0.001*	0.001*	0.001*	0.0001*	0.0001*	0.0001*	0.0001*	0.0001*	0.0001*
DAM - DAM-2	0.044*	0.016*	0.032*	0.023*	0.014*	0.010*	0.006*	0.004*	0.003*
LAM-2 - DAM-2	0.882	0.996	0.562	0.410	0.238	0.164	0.075	0.046*	0.029*

* Statistically significant differences ($p < 0.05$).

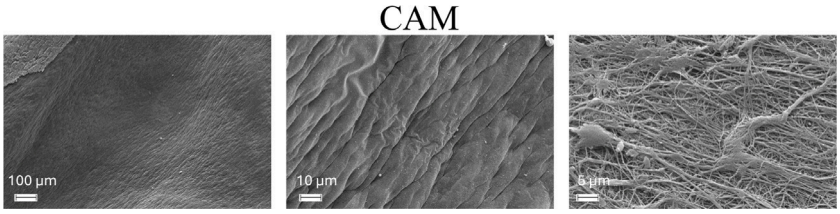

Fig. 5. Representative SEM images of CAM sample at 100×, 1000× and 5000× magnification.

AM, with localized concentrations of salt (NaCl, see Fig. 7). At 1000× magnification, fibers beneath the surface were slightly visible in side A, that probably corresponded to the stromal layer. The lyophilization process caused the sample to be less homogeneous, with overlapped zones characterized by grooves. Fibers were visible at the surface on one side of the LAM sample (side B, 1000× magnification), likely due to the preservation process causing some fibers to rise from the membrane's stroma. Overall, the three membranes displayed a compact and dense structure.

From energy dispersive X-ray spectroscopy, we could check the chemical composition of the membranes. Since the AM samples were identical and only the preservation process differed, we report the EDX analysis of the LAM sample only, to avoid redundancy. Fig. 7 shows the chemical composition obtained with the EDX analysis, by considering three different points of the sample. Point 1 corresponded to the fiber filament, which was found to have the highest concentration of carbon. Point 2 corresponded to a compact homogeneous area, also made of carbon in a lower percentage. Finally, point 3 confirmed the presence of salt, as it was already shown in Fig. 6.

4. Discussion

This study aimed to investigate the effect of different preservation methods on the mechanical behavior of bovine amniotic membranes as well as analyze the associated ultrastructural changes. The three main preservation methods to store AMs before grafting are cryopreservation, lyophilization and dehydration (Jirsova and Jones, 2017). Cryopreservation consists of maintaining the AM at ultra-low temperatures (typically −80 °C or in liquid nitrogen at −196 °C); then, the membranes are stored at −20 °C to prevent the formation of ice crystals that could damage the tissue. In lyophilization, the AM is first frozen, then the water content is removed through sublimation in a vacuum (freeze-drying), leaving a dry, stable product. Finally, in dehydration the AM can be dried using various methods (e.g., air-drying, vacuum drying) to remove moisture while retaining its structural components.

Each preservation method has its own advantages and disadvantages (Jafari et al., 2024). Therefore, the aim of this study arose from the need to evaluate potential alternatives to CAMs, that are currently the most widely used, and to determine whether the preservation methods are interchangeable from a mechanical perspective. Cryopreservation is usually preferred because it maintains the biological properties of the AM, including growth factors and cytokines, and keeps the structural integrity of the ECM and cells intact (Kruse et al., 2000). It also allows long-term storage, but it requires specialized equipment (freezers, liquid nitrogen tanks) and handling procedures, which increase the managing costs and limit its practical use in settings without access to reliable refrigeration (Leal-Marin et al., 2020). The thawing process must be carefully controlled to avoid damaging the tissue and, once thawed, the membrane is difficult to handle as it tends to roll up. Given CAMs' retained bioactivity, they are often used for wound healing and ocular surface reconstruction (Azuara-Blanco et al., 1999). Differently from CAMs, LAMs and DAMs require lower managing costs as they can be stored at room temperature, making it convenient for transport and long-term use. On one hand, lyophilization reduces weight and bulk of the membrane for easier handling with respect to CAM, but some biological properties (e.g., growth factors, cell viability) may be lost during the freeze-drying process (Rodríguez-Ares et al., 2009). Structural integrity may also be compromised due to the freeze-drying dehydration process, though rehydration can restore some properties. As observed with the FE-SEM (Fig. 6), LAM samples appeared to be less homogeneous, with overlapped zones characterized by grooves, probably due to the lyophilization process. However, despite some loss in bioactivity, these membranes still provide a physical

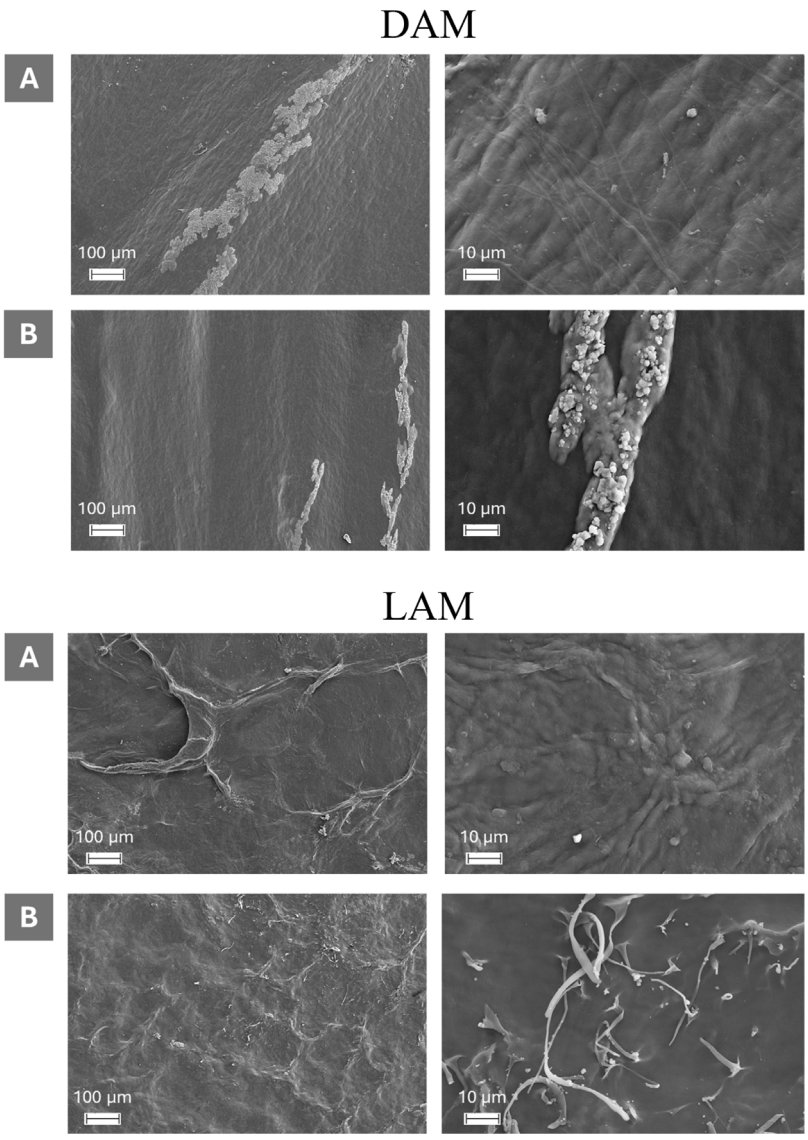

Fig. 6. Representative SEM images of DAM and LAM samples at 100× and 1000× magnification for the two sides of the membranes (A and B).

barrier that promotes epithelialization and protects wounds from infection (Corrêa and Silveira, 2024). Thus, LAMs are often used when ease of storage and transport is essential, such as in wound care products or surgical grafts. On the other hand, DAMs do not require as complex preservation process as CAMs or LAMs. In dehydration, the structural integrity of the ECM is maintained, but the biological activity (such as the presence of growth factors) is typically lower compared to CAMs. In fact, SEM analysis revealed that DAM samples had the most homogeneous and smooth appearance (Fig. 6). DAMs need rehydration before use as LAMs, and the rehydration process might not restore the full functional properties. Therefore, they are typically used in situations where biological activity is less critical, such as providing a physical barrier in wound healing or for tectonic supporting in corneal reconstructive surgery (Castellanos et al., 2017; Costa et al., 2019; Maini et al., 2020).

In our study, statistically significant differences in the mechanical behavior of the three membranes were observed. CAM was the most compliant and had the greatest failure stress. However, as already pointed out, although cryopreservation is the most effective for preserving its biological activity, shrinkage after thawing makes the membrane more difficult to handle and it is also less cost-effective. LAMs and DAMs supported high internal pressures without leakage (up to 200 mmHg) under both protocols and were easier to handle. DAM was stiffer than CAM and LAM in both tests and also felt subjectively stiffer when grasped with forceps. After hydration with the second protocol (samples LAM-2 and DAM-2), both tissues exhibited slightly increased stiffness while still withstanding high pressures without rupture. Despite the structural differences arose among the CAM, LAM and DAM samples observed by SEM due to the different preservation procedures, these differences did not alter or worsen the structural resistance of the AMs, as it was demonstrated with the inflation tests: all samples were able to withstand 5 cycles of 200 mmHg without rupturing or leaking. Thus, from a mechanical perspective the three AMs can all be considered suitable for the repair of stromal to full-thickness corneal defects. Moreover, while LAM and DAM demonstrated superior mechanical performance suggesting greater tectonic support for deeper stromal defects and better handling properties, CAM would also be suitable for corneal repair but preferable when preservation of its biological activity is mandatory.

Two main limitations are assumed in this study. First, while SEM provides insight into the surface micrometric structure of the material, it is insufficient to observe the structure of the membrane in the thickness, thus examination with Transmission Electron Microscope (TEM) would be preferable. Second, the remaining biological activity of the

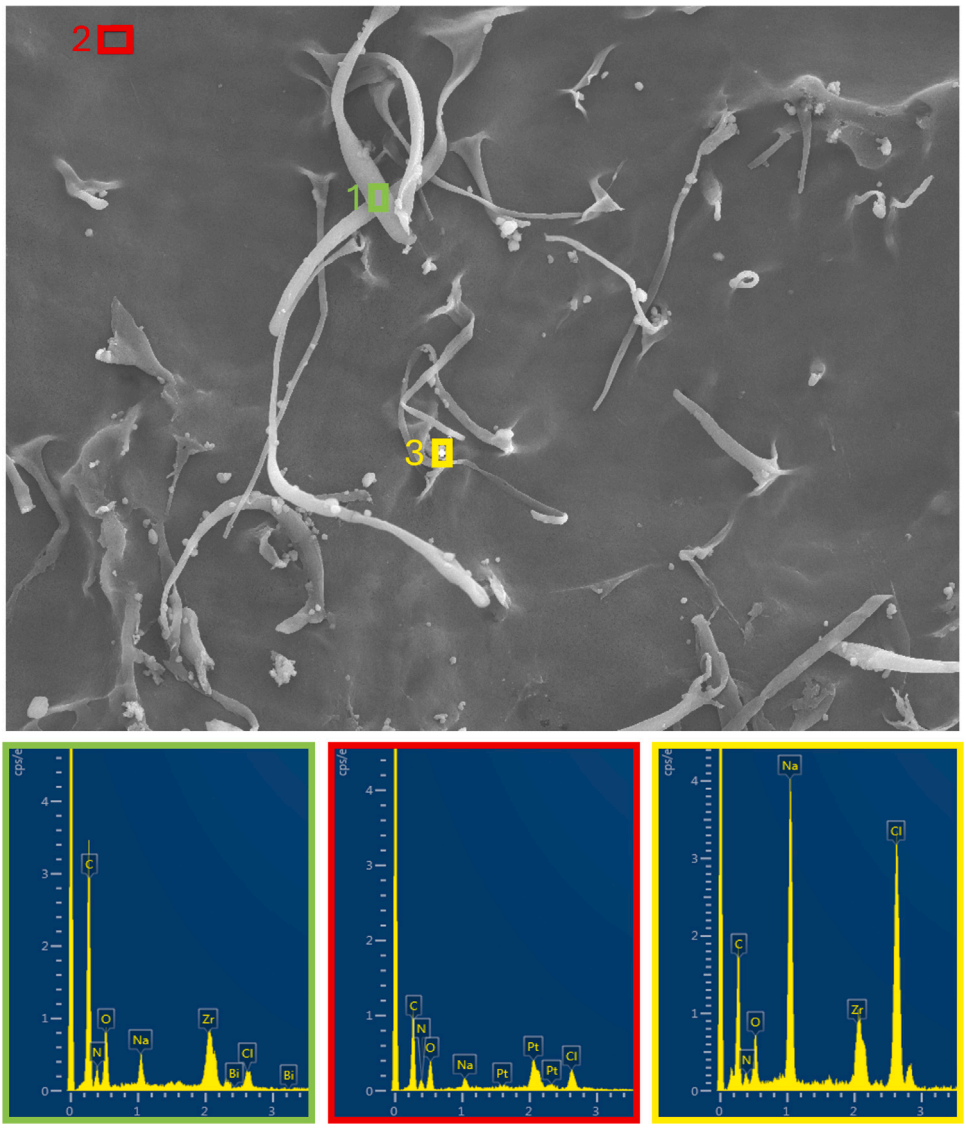

Fig. 7. EDX analysis of the LAM (side B) at 1000× magnification. Three points were selected to examine the chemical composition of the different components of the LAM.

samples after undergoing each preservation method was not evaluated and could not be considered as a parameter for the comparison of the AMs.

Further in vivo studies are warranted to compare the clinical performance of each type of amniotic membrane in corneal defects of variable sizes and depths, and to assess postoperative outcome, potential complications, and corneal transparency, in order to determine which membrane offers more advantages in clinical application. At the same time, future clinical and biomechanical studies focusing on amniotic membranes from various species, along with comparisons to other biomaterials used in corneal surgery, are necessary.

5. Conclusion

Three preservation methods for the conservation of amniotic membranes were evaluated through mechanical tests, SEM examination, and EDX. Although differences in mechanical properties and ultrastructural features of the sample were observed among the methods, none of them compromised the membrane's integrity or strength. Therefore, from a mechanical perspective, the preserved amniotic membranes can be considered functionally equivalent and potentially interchangeable.

CRediT authorship contribution statement

B. Fantaci: Writing – review & editing, Writing – original draft, Software, Methodology, Investigation, Formal analysis, Data curation, Conceptualization. **B. Calvo:** Writing – review & editing, Validation, Supervision, Funding acquisition, Conceptualization. **A.M. Mesa:** Writing – review & editing, Writing – original draft, Visualization, Data curation. **A. Ortillés:** Writing – review & editing, Writing – original draft, Validation, Supervision, Data curation, Conceptualization.

Declaration of competing interest

The authors declare that they have no known competing financial interests or personal relationships that could have appeared to influence the work reported in this paper.

Acknowledgments

The author(s) declare that financial support was received for the research, authorship, and/or publication of this article. This project

has received funding from the European Union's Horizon 2020 research and innovation program under the Marie Skłodowska-Curie grant agreement No 956720 and the Department of Industry and Innovation (Government of Aragon) through the research group Grant T24–23R (cofinanced with Feder 2014–2020: Construyendo Europa desde Aragon). Part of the work was performed by the ICTS "NANBIOSIS" specifically by the High Performance Computing Unit (U27), of the CIBER in Bioengineering, Biomaterials and Biomedicine (CIBER-BBN at the University of Zaragoza-Spain). Finally, the authors would like to acknowledge the use of Servicio General de Apoyo a la Investigación-SAI, Universidad de Zaragoza for SEM image analysis.

Data availability

Data will be made available on request.

References

Allgoewer, I., McLellan, G.J., Agarwal, S., 2010. A keratoprosthesis prototype for the dog. Vet. Ophthalmol. 13, 47–52. http://dx.doi.org/10.1111/j.1463-5224.2009.00759.x.

Andrade, A.L., Laus, J.L., Figueiredo, F., Batista, C.M., 1999. The use of preserved equine renal capsule to repair lamellar corneal lesions in normal dogs. Vet. Ophthalmol. 2, 79–82. http://dx.doi.org/10.1046/j.1463-5224.1999.00052.x.

Andrew, S.E., 2008. Immune-mediated canine and feline keratitis. Vet. Clin.: Small Anim. Pr. 38, 269–290. http://dx.doi.org/10.1016/j.cvsm.2007.11.007.

Arcelli, R., Tibaldini, P., Angeli, G., Bellezza, E., 2009. Equine amniotic membrane transplantation in some ocular surface diseases in the dog and cat: a preliminary study. Vet. Res. Commun. 33, 169–171. http://dx.doi.org/10.1007/s11259-009-9284-6.

Azuara-Blanco, A., Pillai, C.T., Dua, H.S., 1999. Amniotic membrane transplantation for ocular surface reconstruction. Br. J. Ophthalmol. 83, 399–402. http://dx.doi.org/10.1136/bjo.83.4.399.

Baadsgaard Bruun, L., Waskiw Hardon, T.A., Havnsøe Krogh, A.K., Qvortup, K., Heegaard, S., Thuri Kristensen, A., Henriksen, M.L., 2025. The use of a horizontal centrifugation protocol to prepare autologous platelet-rich fibrin membranes for corneal reconstruction surgery in dogs with complicated corneal ulcerations: A case series. Vet. Ophthalmol. 28, 175–189. http://dx.doi.org/10.1111/vop.13148.

Barachetti, L., Giudice, C., Mortellaro, C.M., 2010. Amniotic membrane transplantation for the treatment of feline corneal sequestrum: pilot study. Vet. Ophthalmol. 13, 326–330. http://dx.doi.org/10.1111/j.1463-5224.2010.00821.x.

Barros, P.S., Safatle, A.M., 2000. Congenital scleral staphyloma in a dog repaired with preserved homologous peritoneum. Vet. Ophthalmol. 3, 27–29. http://dx.doi.org/10.1046/j.1463-5224.2000.00102.x.

Barros, P.S., Safatle, A.M., Godoy, C.A., Souza, M.S., Barros, L.F., Brooks, D.E., 2005. Amniotic membrane transplantation for the reconstruction of the ocular surface in three cases. Vet. Ophthalmol. 8, 189–192. http://dx.doi.org/10.1111/j.1463-5224.2005.00391.x.

Braus, B., Miller, I., Kummer, S., Kleinwort, K., Hirmer, S., Hauck, S., McMullen, R., Kerschbaumer, M., Deeg, C., 2017. Investigation of corneal autoantibodies in horses with immune mediated keratitis (immk). Vet. Immunol. Immunopathol. 187, 48–54. http://dx.doi.org/10.1016/j.vetimm.2017.04.002.

Byrd, L.B., Gurnani, B., Martin, N., 2024. Corneal Ulcer. StatPearls Publishing, URL: https://www.ncbi.nlm.nih.gov/books/NBK539689/.

Cassagnes, C., Cognard, S.A., Nicolier, A., Cazalot, G., Dossin, E., Durieux, P., Goulle, F., Michel, J., Pilorge, P., Verneuil, M., Isard, P.F., Mathieson, I., Dulaurent, T., 2020. Corneal epithelial inclusion cysts in 12 dogs (13 eyes) from 2010 to 2019: A multicentric retrospective study. Vet. Ophthalmol. 23, 856–862. http://dx.doi.org/10.1111/vop.12809.

Castellanos, G., Bernabé-García, Á., Moraleda, J.M., Nicolás, F.J., 2017. Amniotic membrane application for the healing of chronic wounds and ulcers. Placenta 59, 146–153. http://dx.doi.org/10.1016/j.placenta.2017.04.005.

Chow, D.W.Y., Westermeyer, H.D., 2016. Retrospective evaluation of corneal reconstruction using acell vet(™) alone in dogs and cats: 82 cases. Vet. Ophthalmol. 19, 357–366. http://dx.doi.org/10.1111/vop.12294.

Corrêa, M.E.A.B., Silveira, P.C.L., 2024. Amniotic membrane in wound healing: New perspectives. J. Wound Care 33, 612–616. http://dx.doi.org/10.12968/jowc.2022.0054.

Costa, D., Leiva, M., Sanz, F., Espejo, V., Esteban, J., Vergara, J., Díaz, C., Huguet, E., Cairó, M., Ríos, J., Peña, M.T., 2019. A multicenter retrospective study on cryopreserved amniotic membrane transplantation for the treatment of complicated corneal ulcers in the dog. Vet. Ophthalmol. 22, 695–702. http://dx.doi.org/10.1111/vop.12643.

Dower, N.M.B., Ribeiro, A.P., Gomes, L.G., de Cássia Martini, A., Taques, I.I.G.G., de Almeida, S.L.H., da Silva, M.I.V., de Aguiar, D.M., 2022. Concentrations of tissue inhibitor of matrix metalloproteinase-1 and hyaluronic acid in canine amniotic membranes cryopreserved for different time points and its effects in dogs with complicated corneal ulcers. Vet. Ophthalmol. 25, 62–72. http://dx.doi.org/10.1111/vop.12916.

Dulaurent, T., Azoulay, T., Goulle, F., Dulaurent, A., Mentek, M., Peiffer, R.L., Isard, P.F., 2014. Use of bovine pericardium (tutopatch®) graft for surgical repair of deep melting corneal ulcers in dogs and corneal sequestra in cats. Vet. Ophthalmol. 17, 91–99. http://dx.doi.org/10.1111/vop.12047.

Gómez, A.P., Mazzucchelli, S., Smith, K., de Lacerda, R.P., 2023. Long-term treatment outcomes and risk factors for recurrence in feline corneal sequestrum: 72 cases (2009–2017). Vet. Rec. 193, e2783. http://dx.doi.org/10.1002/vetr.2783.

Goulle, F., 2012. Use of porcine small intestinal submucosa for corneal reconstruction in dogs and cats: 106 cases. J. Small Anim. Pr. 53, 34–43. http://dx.doi.org/10.1111/j.1748-5827.2011.01149.x.

Hassanpour, K., ElSheikh, R.H., Arabi, A., Frank, C.R., Elhusseiny, A.M., Eleiwa, T.K., Arami, S., Djalilian, A.R., Kheirkhah, A., 2022. Peripheral ulcerative keratitis: A review. J. Ophthalmic Vis. Res. 17, 252–275. http://dx.doi.org/10.18502/jovr.v17i2.10797.

Hoerdemann, M., Yarbrough, T., 2023. Long-term outcome of autologous fascia lata grafting with conjunctival flap overlay in horses with ulcerative keratitis and keratomalacia. Vet. Surg. 52, 1032–1040. http://dx.doi.org/10.1111/vsu.13969.

Jafari, A., Mirzaei, Y., Mer, A.H., Rezaei-Tavirani, M., Jafari, Z., Niknejad, H., 2024. Comparison of the effects of preservation methods on structural, biological, and mechanical properties of the human amniotic membrane for medical applications. Cell Tissue Bank. 25, 305–323. http://dx.doi.org/10.1007/s10561-023-10114-z.

Jirsova, K., Jones, G.L.A., 2017. Amniotic membrane in ophthalmology: properties, preparation, storage and indications for grafting-a review. Cell Tissue Bank. 18, 193–204. http://dx.doi.org/10.1007/s10561-017-9618-5.

Kalpravidh, M., Tuntivanich, P., Vongsakul, S., Sirivaidyapong, S., 2009. Canine amniotic membrane transplantation for corneal reconstruction after the excision of dermoids in dogs. Vet. Res. Commun. 33, 1003–1012. http://dx.doi.org/10.1007/s11259-009-9319-z.

Kanai, K., Kanemaki, N., Matsuo, S., Ichikawa, Y., Okujima, H., Wada, Y., 2006. Excision of a feline limbal melanoma and use of nictitans cartilage to repair the resulting corneoscleral defect. Vet. Ophthalmol. 9, 255–258. http://dx.doi.org/10.1111/j.1463-5224.2006.00452.x.

Kruse, F.E., Joussen, A.M., Rohrschneider, K., You, L., Sinn, B., Baumann, J., Völcker, H.E., 2000. Cryopreserved human amniotic membrane for ocular surface reconstruction. Graefe's Arch. Clin. Exp. Ophthalmol. 238, 68–75. http://dx.doi.org/10.1007/s004170050012.

Lassaline-Utter, M., Gemensky-Metzler, A.J., Scherrer, N.M., Stoppini, R., Latimer, C.A., MacLaren, N.E., Myrna, K.E., 2014. Corneal dystrophy in friesian horses may represent a variant of pellucid marginal degeneration. Vet. Ophthalmol. 17, 186–194. http://dx.doi.org/10.1111/vop.12152.

Leal-Marin, S., Kern, T., Hofmann, N., Pogozhykh, O., Framme, C., Börgel, M., Figueiredo, C., Glasmacher, B., Gryshkov, O., 2020. Human amniotic membrane: A review on tissue engineering, application, and storage. J. Biomed. Mater. Res. Part B: Appl. Biomater. http://dx.doi.org/10.1002/jbm.b.34782.

Ledbetter, E.C., Sanchez, R.F., Repiso, M.L., 2025. Reconstruction of deep and perforating corneal defects in dogs-a review (part ii/iii): Biomaterials and keratoprosthesis. Vet. Ophthalmol. 28, 532–542. http://dx.doi.org/10.1111/vop.13287.

Maini, S., Hurley-Bennett, K., Dawson, C., 2020. Case series describing the use of low-temperature vacuum-dehydrated amnion (omnigen) for the treatment of corneal ulcers in cats and dogs: 46 cases (2016–2017). Top. Companion Anim. Med. 41, 100474. http://dx.doi.org/10.1016/j.tcam.2020.100474.

Malhotra, C., Jain, A.K., 2014. Human amniotic membrane transplantation: Different modalities of its use in ophthalmology. World J. Transplant. 4, 111–121. http://dx.doi.org/10.5500/wjt.v4.i2.111.

Mathes, R.L., Moore, P.A., Ellis, A.E., 2015. Penetrating sclerokeratoplasty and autologous pinnal cartilage and conjunctival grafting to treat a large limbal melanoma in a dog. Vet. Ophthalmol. 18, 152–159. http://dx.doi.org/10.1111/vop.12187.

Mezzadri, V., Crotti, A., Nardi, S., Barsotti, G., 2021. Surgical treatment of canine and feline descemetoceles, deep and perforated corneal ulcers with autologous buccal mucous membrane grafts. Vet. Ophthalmol. 24, 599–609. http://dx.doi.org/10.1111/vop.12907.

Ollivier, F.J., Kallberg, M.E., Plummer, C.E., Barrie, K.P., O'Reilly, S., Taylor, D.P., Gelatt, K.N., Brooks, D.E., 2006. Amniotic membrane transplantation for corneal surface reconstruction after excision of corneolimbal squamous cell carcinomas in nine horses. Vet. Ophthalmol. 9, 404–413. http://dx.doi.org/10.1111/j.1463-5224.2006.00480.x.

Rodríguez-Ares, M.T., López-Valladares, M.J., Touriño, R., Vieites, B., Gude, F., Silva, M.T., Couceiro, J., 2009. Effects of lyophilization on human amniotic membrane. Acta Ophthalmol. 87, 396–403. http://dx.doi.org/10.1111/j.1755-3768.2008.01261.x.

Ruiz-Lozano, R.E., Ramos-Davila, E.M., Garza-Garza, L.A., Gutierrez-Juarez, K., Hernandez-Camarena, J.C., Rodriguez-Garcia, A., 2023. Rheumatoid arthritis-associated peripheral ulcerative keratitis outcomes after early immunosuppressive therapy. Br. J. Ophthalmol. 107, 1246–1251. http://dx.doi.org/10.1136/bjophthalmol-2022-321132.

Sanchez, R.F., Ledbetter, E.C., Leiva, M., 2024. Reconstruction of deep and perforating corneal defects in dogs-a review (part i/iii): Autogenous ocular tissues, donor tissues, and corneal clarity scoring. Vet. Ophthalmol. 28, 519–531. http://dx.doi.org/10.1111/vop.13286.

Santillo, D., Mathieson, I., Corsi, F., Göllner, R., Guandalini, A., 2021. The use of acellular porcine corneal stroma xenograft (biocorneavet™) for the treatment of deep stromal and full thickness corneal defects: A retrospective study of 40 cases (2019–2021). Vet. Ophthalmol. 24, 469–483. http://dx.doi.org/10.1111/vop.12927.

Stapleton, F., 2023. The epidemiology of infectious keratitis. Ocul. Surf. 28, 351–363. http://dx.doi.org/10.1016/j.jtos.2021.08.007.

Thajunnisa, A.S., Sainulabdeen, A., Dileepkumar, K.M., Philip, L.M., Vasudevan, V.N., Devanand, C.B., 2020. Comparative evaluation of decellularized bovine omentum alone and in combination with mitomycin-c in the management of corneal injuries in dogs. Vet. World 13, 2401–2410. http://dx.doi.org/10.14202/vetworld.2020.2401-2410.

Vicenti, F.A., Laus, J.L., Costa Neto, J.M., Talieri, I.C., Campos, C.F., Jorge, A.T., Ferreira, A.L., Fantinatti, A.P., 2003. Effects of low-intensity pulsed ultrasound on wound healing in corneas of dogs following keratoplasty. Vet. Ophthalmol. 6, 255–263. http://dx.doi.org/10.1046/j.1463-5224.2003.00303.x.

Zhang, L., Zou, D., Li, S., Wang, J., Qu, Y., Ou, S., Jia, C., Li, J., He, H., Liu, T., Yang, J., Chen, Y., Liu, Z., Li, W., 2016. An ultra-thin amniotic membrane as carrier in corneal epithelium tissue-engineering. Sci. Rep. 6 (21021), http://dx.doi.org/10.1038/srep21021.